Supplementary Information: Quantitative measurement of microbial growth with Raman microspectroscopy

Tristan A. Caro[1], Srishti Kashyap[1], George Brown[2], Claudia Chen[2], Sebastian Kopf[1], Alexis Templeton[1]

1. Department of Geological Sciences, University of Colorado Boulder. Boulder CO, USA
2. Laboratory for Interdisciplinary Statistical Analysis, University of Colorado Boulder. Boulder CO, USA

This file includes:

- Supplementary Text
- Supplementary Figures S1 - S#
- Supplementary References

1 Supplementary Text

1.1 Correlation between Raman and nanoSIMS measurements

Given the observed depression in deuterium abundance measured by nanoSIMS, we sought to understand whether it would be feasible to correct future nanoSIMS D/H values by establishing a relationship to Raman-derived D/H values. To enable this, we examined the correlation between Raman- and nanoSIMS-derived ${}^{2}F$ values. We applied linear modeling bootstrapping analysis and found that strong correlation was demonstrated between Raman and nanoSIMS ${}^{2}F$ (adjusted $R^2 = 0.8239$). Our model tested across both cell types and yielded a residual standard error of 2.49 % on 349 degrees of freedom ($F = 1639$ on 1 and 349 DF, $p < 2.2E\text{-}16$). Using the model fit on the training set to predict the testing set yielded a root mean squared error (RMSE) of 2.54 %, which represents the difference, on average, between actual and predicted values (**Main Text, Table 1D**). We therefore conclude that correcting nanoSIMS

values by conversion to undiluted "Raman-equivalents" is tractable. However, this conversion introduces an additional source of uncertainty that, as with applying a single dilution factor, should be accounted for in downstream calculations, and may be unacceptable for reasonable estimation of growth rate.

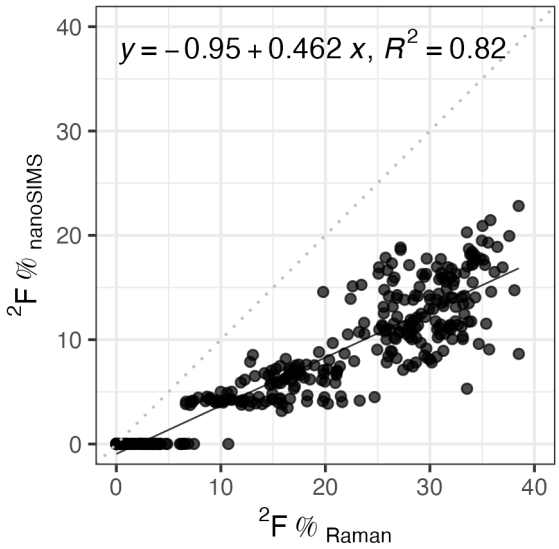

Figure S1. The relationship of cellular deuterium enrichment between Raman- and nanoSIMS-derived measurements.

1.2 Growth rate error propagation

Uncertainty in growth rate measurements (σ_μ) depends on uncertainty in each parameter of the growth rate calculation:

$$\mu = -\frac{1}{t} ln(\frac{F_T - a \cdot F_L}{F_0 - a \cdot F_L})$$

We propagated error of individual parameters according to (1) to uncertainty in growth rate using standard propagation of uncertainty via partial derivatives, assuming all measurements to be uncorrelated ####FIX:

$$\sigma_\mu = \frac{(aF_L - F_T)^2 \sigma_{F_0}^2}{t \cdot (aF_L - F_0) \cdot (aF_L - F_T)}$$

For the purposes of this work, we exclude the uncertainty in SIP incubation time (t) as we assume that this quantity is negligible for SIP incubations that last multiple days ($\sigma_T = 0$) .

We advise future researchers using rapidly growing organisms and short incubation times to estimate and include this value.

1.3 Surface-enhanced Raman spectroscopy

Surface-enhanced Raman spectroscopy (SERS) is a methodology that employs the adsorption of metal ions (e.g., Ag, Au, Cu, Zn, etc.) to a target substrate (2,3) in order to enhance Raman scattering effects. Surface enhancement with modern SERS methodologies have resulted in signal enhancements up to 10^5 – 10^6 (2). Therefore, we hypothesized that SERS could be a useful technique in dramatically increasing the sensitivity of Raman spectroscopy for the detection of deuterium in microbial biomass.

To this end, we synthesized silver nanoparticles (AgNPs) using the trisodium citrate reduction method adapted from (4–6). AgNPs were synthesized by dissolving 72mg of AgNO3 in 400mL ultrapure water (18.2 MΩ cm) in an Erlenmeyer flask. The solution was heated to initial boiling (~90 $^\circ$C) under vigorous stirring. 8mL of 1% wt/vol trisodium citrate solution was slowly added into the reaction flask and the combined solution was allowed to boil for approximately one hour. Once the solution had turned an apparent luminescent yellow, the solution was allowed to cool to room temperature. The average diameter of AgNPs in suspension was calorimetrically determined to be 50 nm, as the absorption max was 420nm (7). AgNPs were mixed with sulfate reducing bacteria (SRB) *T. hydrogeniphilus* (See Main Text: Materials and Methods: Biological Sample Preparation). A cell pellet from the SRB culture was mixed directly with 10µL of concentrated AgNPs and mixed by gentle pipetting, and spotted onto an aluminum-coated glass slide, and allowed to air-dry prior to Raman spectroscopy.

{need methods here on the Raman parameters used for SERS}

We observed substantial signal enhancement in the fingerprint region on the order of ##### with the addition of AgNPs. We note that the acquisition time and laser power required acquisition of cell spectra using SERS is significantly reduced when compared to the normal methodology (See Main Text: Materials and Methods). We note two key observations that we believe warrant caution when applying SERS methodology to microbial samples.

The first, most crucial observation, is the lack of signal enhancement in the higher wavenumber regions corresponding to the organic CH and CD bands. It is known that a SERS spectra is determined by the molecular species in close association to adsorbed AgNPs on the cell surface. We hypothesize that, because AgNPs preferentially nucleate around highly-functionalized molecules such as fused-ring systems, flavins, nucleic acids, etc. (8), signal enhancement of C-H bonds is weak or non-existent. Second, we noticed that signal enhancement was uneven (previously observed (8)) and changes over time with multiple acquisitions. While SERS allows the acquisition of cell spectra in mere seconds, it also produces spurious, ephemeral spectral artifacts, including "ghost peaks" that appeared and disappeared, peak position shifts, and graphitization of the cell. We conclude that SERS methodologies, which have been applied with impressive success for purposes of materials characterization, single molecule detection,

and molecular characterization, are promising for microbiological characterization. However, more fundamental, mechanistic work is required before it can be robustly applied to environmental systems or to accurately detect and quantify hydrogen isotopic changes.

1.4 NanoSIMS dilution factor calculations

Dilution of isotopic signal by sample preparation for nanoSIMS has been widely observed ((9–13)). Here we define the dilution factor of sample preparation (D) similar to (14):

$$D = \frac{F_{after} - F_{before}}{F_{added} - F_{before}}$$

where F denotes isotope fraction (at. %) of biomass before and after sample preparation, as well as that of the diluent material (F_{added}). Here, we take the Raman-derived $\^2F$ as the *before* value, the nanoSIMS as the *after* value, and natural abundance hydrogen as the *added* value. Because the natural abundance of deuterium is negligible in comparison to the label strengths used for this study, we set $F_{added} = 0.00015\%$ (VSMOW). Here we make explicit the assumption that the Raman-derived value, calculated from CD%, is approximate to whole-cell isotopic composition *before* cell washing. In other words, we assume that molecules incorporate deuterium equally towards non-exchangeable C-H bonds (measurable by Raman) as protic sites in cellular biomass (measurable by nanoSIMS).

We calculated uncertainty in dilution factor using standard propagation of uncertainty via partial derivatives, assuming all measurements to be uncorrelated. This uncertainty term is calculated to be:

$$\sigma_D = \sqrt{\left(\frac{1}{F_{added} - F_{before}} \cdot \sigma_{F_{after}}\right)^2 + \left(\frac{F_{after} - F_{added}}{(F_{added} - B)^2} \cdot \sigma_{F_{before}}\right)^2 + \left(\frac{F_{before} - F_{after}}{(F_{added} - F_{before})^2} \cdot \sigma_{F_{added}}\right)^2}$$

For future researchers: back-calculation of the isotopic composition of biomass *before* sample preparation can be done by rearrangement of the dilution factor equation, solving for F_{before}:

$$F_{before} = \frac{F_{after} - (F_{added} \cdot DF)}{1 - DF}$$

The propagated uncertainty in this equation is therefore:

$$\sigma_{F_{before}} = \sqrt{\left(\frac{1}{1-D} \cdot \sigma_{F_{after}}\right)^2 + \left(-\frac{D}{1-D} \cdot \sigma_{F_{added}}\right)^2 + \left(\frac{F_{after} - F_{added}}{(1-D)^2} \cdot \sigma_D\right)^2}$$

1.5 Effect of dead time correction on nanoSIMS-derived data

We observed a negligible effect of dead time correction (Main Text: Materials and Methods) on deuterium isotopic abundances. The maximum deadtime effect was observed at higher deuterium abundance. The maximum residual difference between raw and dead-time corrected (DTC) nanoSIMS data was just under 0.05 at. %, with most residuals below 0.03 at. %. Given that our labeling enrichment varied between 0 - 50 at. %, we consider this a negligible effect.

1.5.1 Figure S2

(A) The difference in ${}^2F$ between raw and dead time-corrected (DTC) values. Points are ordered in descending order from greatest difference between raw and DTC value. The top panel indicates relative frequency of observations, differentiated by $2F_{label}$. (B) The difference in ${}^2F$ between raw and DTC values increases with increasing ${}^2F$. Residual differences in raw and DTC values are negligible compared to the magnitude of the $2F$ values reported here. ${}^2F$ values near natural-abundance exhibited miniscule effects related to dead time correction. (C) Raw and DTC ${}^2F$ values plotted against each other, with a linear fit (red).

1.6 Supplementary Datasets

Dataset S1 (separate file).

Dataset S2 (separate file).

2 Supplementary References

.

1. Caro TA, McFarlin J, Jech S, Fierer N, Kopf S. Hydrogen stable isotope probing of lipids demonstrates slow rates of microbial growth in soil. Proceedings of the National Academy of Sciences [Internet]. 2023 Apr 18;120(16):e2211625120. Available from: https://www.pnas.org/doi/10.1073/pnas.2211625120

2. Langer J, Jimenez de Aberasturi D, Aizpurua J, Alvarez-Puebla RA, Auguié B, Baumberg JJ, et al. Present and future of surface-enhanced raman scattering. ACS Nano [Internet]. 2020 Jan 28;14(1):28–117. Available from: https://doi.org/10.1021/acsnano.9b04224

3. Cui L, Yang K, Zhu YG. Stable Isotope-Labeled Single-Cell Raman Spectroscopy Revealing Function and Activity of Environmental Microbes. In: Dumont MG, Hernández García M, editors. New York, NY: Springer; 2019. p. 95–107. (Methods in Molecular Biology). Available from: https://doi.org/10.1007/978-1-4939-9721-3_8

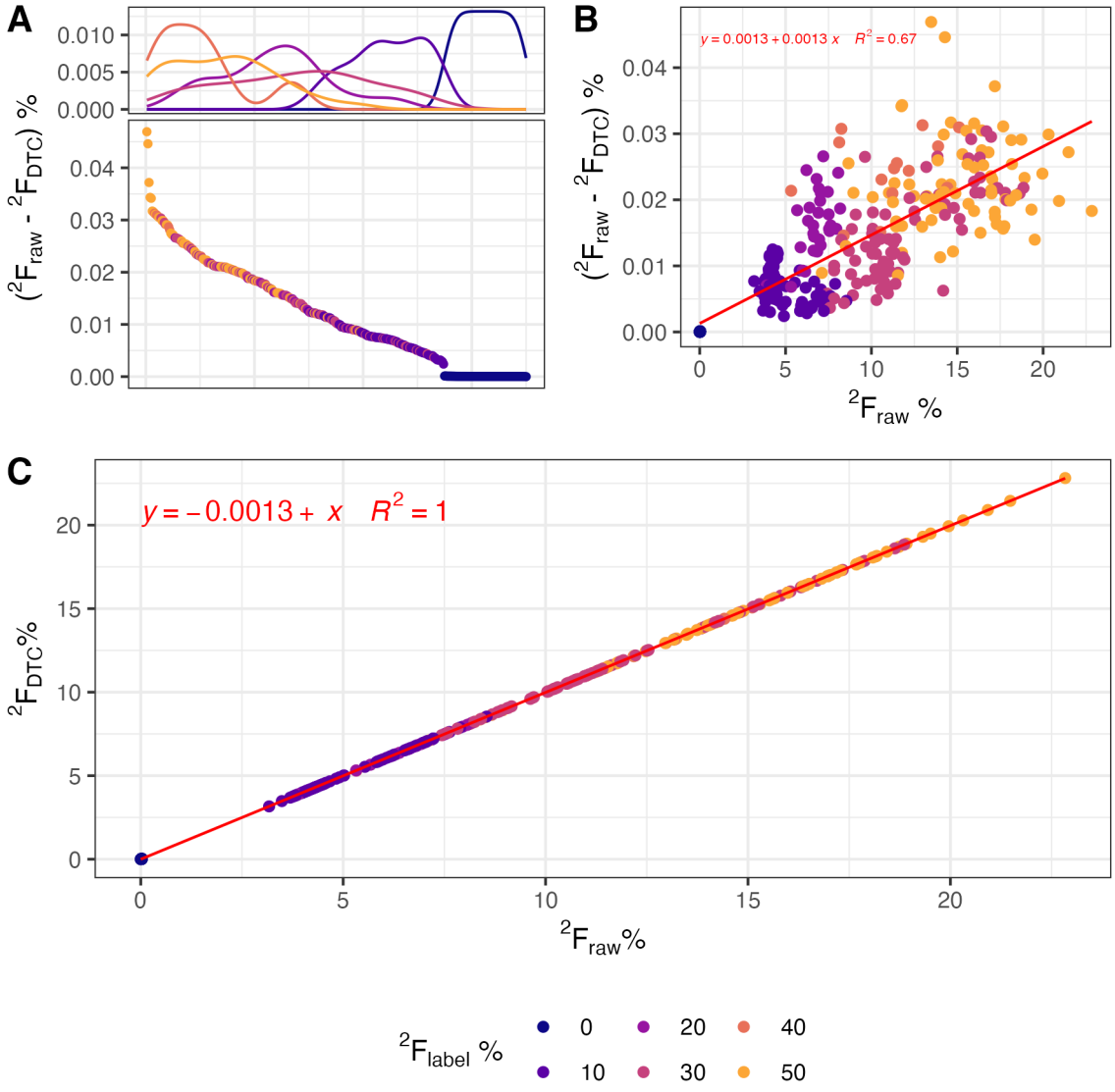
A
B
C
$^2F_{raw}$ - $^2F_{DTC}$) %
$^2F_{raw}$ %
$^2F_{DTC}$%
$^2F_{raw}$%
$y = 0.0013 + 0.0013\ x$ $R^2 = 0.67$
$y = -0.0013 + x$ $R^2 = 1$
$^2F_{label}$ %
0
10
20
30
40
50

4. Cui L, Yang K, Zhu YG. Stable Isotope-Labeled Single-Cell Raman Spectroscopy Revealing Function and Activity of Environmental Microbes. In: Dumont MG, Hernández García M, editors. New York, NY: Springer; 2019. p. 95–107. (Methods in Molecular Biology). Available from: https://doi.org/10.1007/978-1-4939-9721-3_8

5. Mulfinger L, Solomon SD, Bahadory M, Jeyarajasingam AV, Rutkowsky SA, Boritz C. Synthesis and Study of Silver Nanoparticles. Journal of Chemical Education [Internet]. 2007 Feb;84(2):322. Available from: https://pubs.acs.org/doi/abs/10.1021/ed084p322

6. Lee PC, Meisel D. Adsorption and surface-enhanced Raman of dyes on silver and gold sols [Internet]. 2002. Available from: https://pubs.acs.org/doi/pdf/10.1021/j100214a025

7. Paramelle D, Sadovoy A, Gorelik S, Free P, Hobley J, G. Fernig D. A rapid method to estimate the concentration of citrate capped silver nanoparticles from UV-visible light spectra. Analyst [Internet]. 2014;139(19):4855–61. Available from: https://pubs.rsc.org/en/content/articlelanding/2014/an/c4an00978a

8. Efrima S, Zeiri L. Understanding SERS of bacteria. Journal of Raman Spectroscopy [Internet]. 2009;40(3):277–88. Available from: https://onlinelibrary.wiley.com/doi/abs/10.1002/jrs.2121

9. Kopf SH, McGlynn SE, Green-Saxena A, Guan Y, Newman DK, Orphan VJ. Heavy water and 15N labelling with NanoSIMS analysis reveals growth rate-dependent metabolic heterogeneity in chemostats. Environmental Microbiology [Internet]. 2015;17(7):2542–56. Available from: https://onlinelibrary.wiley.com/doi/abs/10.1111/1462-2920.12752

10. Musat N, Stryhanyuk H, Bombach P, Adrian L, Audinot JN, Richnow HH. The effect of FISH and CARD-FISH on the isotopic composition of 13C- and 15N-labeled Pseudomonas putida cells measured by nanoSIMS. Systematic and Applied Microbiology [Internet]. 2014 Jun 1;37(4):267–76. Available from: https://www.sciencedirect.com/science/article/pii/S072320201400037X

11. Pernice M, Dunn SR, Tonk L, Dove S, Domart-Coulon I, Hoppe P, et al. A nanoscale secondary ion mass spectrometry study of dinoflagellate functional diversity in reef-building corals. Environmental Microbiology [Internet]. 2015;17(10):3570–80. Available from: https://onlinelibrary.wiley.com/doi/abs/10.1111/1462-2920.12518

12. Stryhanyuk H, Calabrese F, Kümmel S, Musat F, Richnow HH, Musat N. Calculation of single cell assimilation rates from SIP-NanoSIMS-derived isotope ratios: A comprehensive approach. Frontiers in Microbiology [Internet]. 2018;9. Available from: https://www.frontiersin.org/articles/10.3389/fmicb.2018.02342

13. Woebken D, Burow LC, Behnam F, Mayali X, Schintlmeister A, Fleming ED, et al. Revisiting N2 fixation in Guerrero Negro intertidal microbial mats with a functional single-cell approach. The ISME Journal [Internet]. 2015 Feb;9(2):485–96. Available from: https://www.nature.com/articles/ismej2014144

14. Meyer NR, Fortney JL, Dekas AE. NanoSIMS sample preparation decreases isotope enrichment: magnitude, variability and implications for single-cell rates of microbial activity. Environmental Microbiology [Internet]. 2021;23(1):81–98. Available from: https://onlinelibrary.wiley.com/doi/abs/10.1111/1462-2920.15264